Structure-Based Design, Synthesis, and Biological Evaluation of Conformationally Restricted Novel 2-Alkylthio-6-[1-(2,6-difluorophenyl)alkyl]-3,4-dihydro-5-alkylpyrimidin-4(3*H*)-ones as Non-nucleoside Inhibitors of HIV-1 Reverse Transcriptase

Antonello Mai,[†] Gianluca Sbardella,[†] Marino Artico,*[,†] Rino Ragno,[‡] Silvio Massa,[§] Ettore Novellino,[||] Giovanni Greco,[||] Antonio Lavecchia,[||] Chiara Musiu,[⊥] Massimiliano La Colla,[#] Chiara Murgioni,[#] Paolo La Colla,*[,#] and Roberta Loddo[#]

Istituto Pasteur-Fondazione Cenci Bolognetti, Dipartimento di Studi Farmaceutici, Università degli Studi di Roma "La Sapienza", P.le A. Moro 5, I-00185 Roma, Italy, Dipartimento di Studi di Chimica e Tecnologie delle Sostanze Biologicamente Attive, Università degli Studi di Roma "La Sapienza", P.le A. Moro 5, I-00185 Roma, Italy, Dipartimento Farmaco Chimico Tecnologico, Università degli Studi di Siena, via Aldo Moro, I-53100 Siena, Italy, Dipartimento di Chimica Farmaceutica e Tossicologica, Università degli Studi di Napoli "Federico II", Via D. Montesano 49, I-80131 Napoli, Italy, Novirio Pharmaceuticals, Inc., Boston, and Dipartimento di Biologia Sperimentale, Sezione di Microbiologia, Università degli Studi di Cagliari, Cittadella Universitaria SS 554, I-09042 Monserrato (Cagliari), Italy

Received February 26, 2001

5-Alkyl-2-(alkylthio)-6-(2,6-difluorobenzyl)-3,4-dihydropyrimidin-4(3*H*)-ones (*S*-DABOs, **2**) have been recently described as a new class of human immunodeficiency virus type 1 (HIV-1) non-nucleoside reverse transcriptase (RT) inhibitors (NNRTIs) active at nanomolar concentrations (Mai, A. et al. *J. Med. Chem.* **1999**, *42*, 619−627). In pursuing our lead optimization efforts, we designed novel conformationally restricted *S*-DABOs, **3**, featuring a methyl at the benzylic carbon (Y = Me) and at the pyrimidine 5-position (R = Me). Conformational analyses and docking simulations suggested that the presence of both methyls would significantly reduce conformational flexibility without compromising, in the *R* enantiomers, the capability of fitting into the RT non-nucleoside binding pocket. To develop structure−activity relationships, we prepared several congeners of type **3** belonging to the thymine (R = Me) and uracil (R = H) series, featuring various 2-alkylthio side chains (X = Me, *i*-Pr, *n*-Bu, *i*-Bu, *s*-Bu, *c*-pentyl, and *c*-hexyl) and aryl moieties different from the 2,6-difluorophenyl (Ar = phenyl, 2,6-dichlorophenyl, 1-naphthyl). Moreover, α-ethyl derivatives (Y = Et) were included in the synthetic project in addition to α-methyl derivatives (Y = Me). All of the new compounds were evaluated for their cytotoxicity and anti-HIV-1 activity in MT-4 cells, and some of them were assayed against highly purified recombinant wild-type HIV-1 RT using homopolymeric template primers. The results were expressed as CC_{50} (cytotoxicity), EC_{50} (anti-HIV-1 activity), SI (selectivity, given by the CC_{50}/EC_{50} ratio), and IC_{50} (RT inhibitory activity) values. In the 2,6-difluorobenzylthymine (R = Me) series, methylation of the benzylic carbon improved anti-HIV-1 and RT inhibitory activities together with selectivity. Compound **3w** (Ar = 2,6-F_2-Ph, R = Y = Me, X = *c*-pentyl) turned out the most potent and selective among the *S*-DABOs reported to date (CC_{50} > 200 μM, EC_{50} = 6 nM, IC_{50} = 5 nM, and SI > 33 333). Assays performed on the pure enantiomer (+)-**3w**, much more active than (−)-**3w**, yielded the following results: CC_{50} > 200 μM, EC_{50} = 2 nM, IC_{50} = 8 nM, and SI > 100 000, under conditions wherein MKC-442 was less active and selective (CC_{50} > 200 μM, EC_{50} = 30 nM, IC_{50} = 40 nM, SI > 6666). The 2,6-difluorophenylethylthymines (R = Me) were generally endowed with higher potency compared with the uracil counterparts (R = H). In the 2,6-difluorophenyl series the best and the least performant 2-alkylthio side chains were the 2-*c*-pentylthio and the 2-methylthio, respectively. When the methyl at the benzylic carbon was replaced by an ethyl, activity was retained or decreased slightly, thus suggesting that the dimensions of the cavity within the RT hosting this substituent would not be compatible with groups larger than ethyl. Aryl moieties different from the 2,6-difluorophenyl (phenyl, 1-naphthyl, 2,6-dichlorophenyl) were generally detrimental to activity, consistent with a favorable electronic effect exerted by the 2,6-fluorines on a putative charge-transfer interaction between the aromatic moieties of the inhibitor and Tyr188.

Introduction

The human immunodeficiency virus type 1 (HIV-1) reverse transcriptase (RT) is a multifunctional enzyme responsible for the conversion of single-stranded RNA viral genome to double-stranded DNA.[1−3] Two distinct

* To whom correspondence should be addressed. For M.A.: phone and fax, +39064462731; e-mail, marino.artico@uniroma1.it. For P.L.C.: phone, +390706754147; fax, +390706754210; e-mail, placolla@unica.it.
[†] Dipartimento di Studi Farmaceutici, Università degli Studi di Roma "La Sapienza".
[‡] Dipartimento di Studi di Chimica e Tecnologie delle Sostanze Biologicamente Attive, Università degli Studi di Roma "La Sapienza".
[§] Università degli Studi di Siena.
[||] Università degli Studi di Napoli "Federico II".
[⊥] Novirio Pharmaceuticals, Inc.
[#] Università degli Studi di Cagliari.

10.1021/jm010853h CCC: $20.00 © 2001 American Chemical Society
Published on Web 07/10/2001

Chart 1. Structures of Well-Known RT Inhibitors

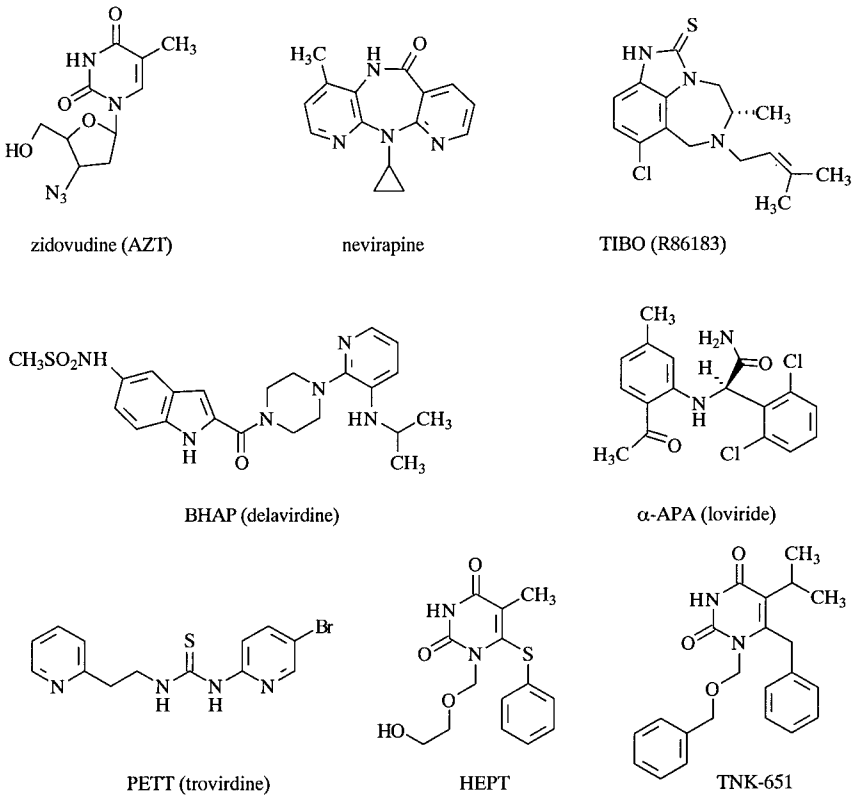

classes of RT inhibitors are currently being used in the treatment of AIDS: the nucleoside (NRTIs) and non-nucleoside (NNRTIs) inhibitors (Chart 1). The NRTIs, whose prototype is zidovudine,[4] are phosphorylated and act competitively at the catalytic site of the enzyme as DNA chain-terminating analogues of the natural deoxynucleoside triphosphates.[5] However, their therapeutic effectiveness is limited by toxicity, unfavorable pharmacokinetics, and emergence of resistant viral strains.[6−8] NNRTIs comprise many structurally diverse compounds such as nevirapine,[9] TIBO,[10] BHAP,[11] α-APA,[12] PETT,[13] HEPT,[14] and TNK-651.[15] Crystal structures of several RT/inhibitor complexes[15−23] clearly show that NNRTIs share a common mode of action, binding to an allosteric site located about 10 Å from the catalytic site. Although these agents generally exhibit low toxicity and favorable pharmacokinetic properties, resistant viral populations rapidly develop following their administration.[24,25] Therefore, there is still a need to identify new NNRTIs endowed with high inhibitory activity against wild-type RT as well as its clinically relevant mutants.[26]

Dihydroalkoxybenzyloxopyrimidines (DABOs, **1**), structurally related to HEPT, were disclosed as NNRTIs by our group in 1993.[27−29] Since then, we have been performing many structural modifications on DABO lead compounds with the aim of improving potency.[30,31] The most fruitful result of these efforts was the discovery of 2,6-difluorobenzyl-*S*-DABO derivatives (**2**)[32] active at nanomolar concentrations in cell-based and enzymatic assays. Compounds **2** were designed prompted by computational studies suggesting that 2,6-dihalogenation of the *S*-DABO phenyl moiety would enhance a charge-transfer interaction between the π-stacking aromatic rings of the ligand and Tyr188.

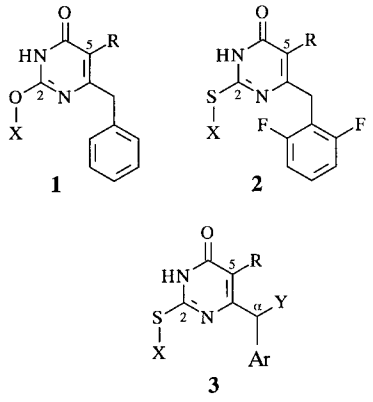

In pursuing our lead optimization efforts, we have recently investigated novel *S*-DABOs of general formula **3** as conformationally restricted analogues of the 2,6-difluorobenzyl-*S*-DABOs **2**. The present paper describes the design, the synthesis, biological evaluation, and the structure−activity relationships (SARs) of compounds **3**.

Computer-Aided Design

A typical strategy to improve potency of a lead compound is to synthesise conformationally restricted analogues with at least one conformation, among a few energetically allowed conformations, recognized by the target. Structural modifications of previously reported 2,6-difluorobenzyl-*S*-DABOs **2**[32] were therefore sought to reduce flexibility without producing any steric misfit between the ligands and the RT non-nucleoside binding cleft. This problem was approached using computational tools as herein summarized (procedures are detailed in the Experimental Section).

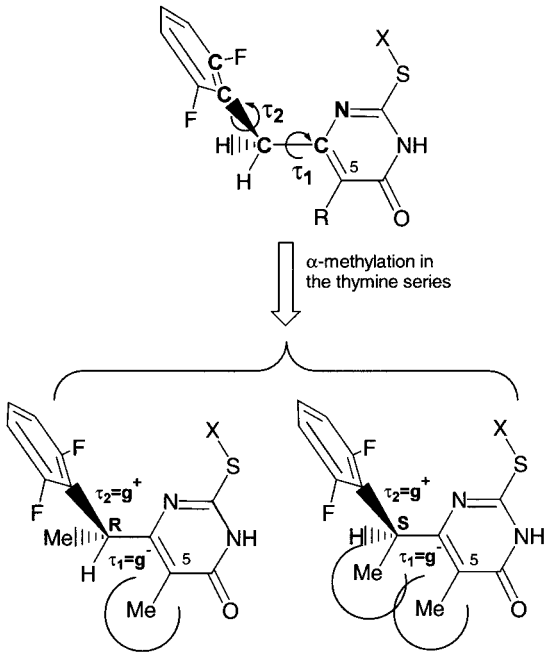

Figure 1. Torsion angles τ_1 and τ_2 are defined by the atoms in bold (top). Effects of α-methylation and chirality on stability of the [g⁻,g⁺] conformation in the thymine series (R = Me) of 2,6-difluorobenzyl-*S*-DABOs are shown (bottom).

A variety of different conformations are accessible to the 2,6-difluorobenzyl side chain of compounds **2** because of rotation around the two bonds connecting the pyrimidine and the 2,6-difluorophenyl rings. Each conformation is univocally identified through the torsion angles τ_1 and τ_2 defined in Figure 1. Docking studies performed in our laboratories[32,33] suggested that the RT-bound conformation of these molecules is characterized by a gauche⁻, gauche⁺ (g⁻, g⁺) arrangement about τ_1 and τ_2, respectively (Figure 1). Insertion of a methyl group on the benzylic carbon of 2,6-difluorobenzyl-5-methyl-*S*-DABOs (thymine series) selects or destabilizes conformations of the [g⁻,g⁺] family depending on whether the configuration is *R* or *S*, respectively. In fact, while in the *R* enantiomer the α-methyl points outward from thymine 5-methyl, in the *S* enantiomer the two methyl groups are eclipsed and sterically repel each other (Figure 1).

Conformational analyses were performed on four 2,6-difluorobenzyl-*S*-DABO models[34] differing in the presence or absence of a methyl at the pyrimidine 5-position and the benzylic carbon with *R* configuration. The results are summarized in Figure 2 as scatter plots in the plane of τ_1 and τ_2. In these diagrams, a conformation is labeled with a circle ("low energy") or a cross depending on whether its strain energy (E_{strain}) is within or above 2 kcal/mol. E_{strain} was calculated as the difference in energy with respect to the global minimum conformation. Expectedly, the number of low-energy conformations reaches a minimum when both methyls are present: only seven low-energy conformations of [g⁻,g⁺] type out of the 180 generated. A single methyl decreases flexibility to a lesser extent compared with the desmethyl counterpart: 39 or 41 vs 72 low-energy conformations.

To verify whether, among the conformation of [g⁻,g⁺] type selected by the (*R*)-α-methyl group, there was any recognized by RT, the *S*-DABO (*R*)-**3w** (Ar = 2,6-F_2-Ph, R = Y = (*R*)-Me, X = *c*-pentyl) was docked into the non-nucleoside binding pocket of the target enzyme. The docking calculations differed in some methodological aspects from those described in a previous paper.[32] Particularly, the structure of RT that cocrystallized with TNK-651[15] (unavailable at the time we designed the first 2,6-difluorobenzyl-*S*-DABOs) was selected to take into account a conformational change induced onto the Tyr181 side chain by highly potent inhibitors. Our previous models were in fact based on the coordinates of the RT/HEPT complex[16] wherein the Tyr181 side chain is not "switched on". Moreover, a more rigorous computational procedure was applied on the basis of the Amber force field parametrization[35,36] and molecular dynamics (MD) calculations.

Throughout the 500 ps MD simulation of the RT/(*R*)-**3w** complex, τ_1 and τ_2 fluctuated within g⁻ and g⁺ ranges centered on mean values of −51° and 87°. Figure 3 shows the model obtained by energy-minimizing the structure of the complex averaged over the last 100 ps. The RT-bound conformation of the ligand is characterized by a "propeller-like" disposition of the thymine and the 2,6-difluorophenyl rings with $\tau_1 = -47°$ and $\tau_2 = 88°$. These values correspond to a family of conformations stabilized by the (*R*)-α-methyl group (highlighted by an arrow in Figure 2). The pyrimidine NH−C═O moiety is engaged in two hydrogen bonds with the Lys101 C═O and NH, respectively. The 2,6-difluorophenyl ring contacts favorably the Tyr181 side chain, giving rise to a π-stacking interaction. The 2-*c*-pentylthio substituent fits into the Pro236 hairpin pocket.[15] Finally, the α-methyl group is well accommodated in a small cavity made up of Val179 side chain and Tyr181 plus Tyr188 main chains.

The results of the conformational analyses and docking simulations gave support to the preparation and biological evaluation of conformationally restricted α-methyl-2,6-difluorobenzyl-*S*-DABOs such as compound **3w**. To develop SARs, we planned the synthesis of various congeners of general formula **3** belonging to either the thymine (R = Me) and uracil (R = H) series, featuring various 2-alkylthio side chains (X = Me, *i*-Pr, *n*-Bu, *i*-Bu, *s*-Bu, *c*-pentyl, and *c*-hexyl) and aryl moieties different from the 2,6-difluorophenyl (Ar = phenyl, 2,6-dichlorophenyl, 1-naphthyl). To probe the dimensions of the cavity within RT hosting the substituent on the benzylic carbon, α-ethyl derivatives (Y = Et) were included in the synthetic project in addition to α-methyl derivatives (Y = Me).

Chemistry

The synthesis of the title compounds was accomplished by two alternative routes: (i) preparation of 6-(1-arylethyl)- and 6-(1-arylpropyl)-3,4-dihydro-2-thioxopyrimidin-4(3*H*)-ones (**6**) followed by S-alkylation in dry DMF with the appropriate haloalkane in the presence of potassium carbonate to afford **3a**−**j**, **s**, **u**−**x**, **a′**−**j′** (Scheme 1) and (ii) direct lithiation of 2-alkylthio-6-(2,6-difluorobenzyl)-3,4-dihydropyrimidin-4(3*H*)-ones at 0 °C with lithium diisopropylamide (LDA) in dry THF and hexamethylphosphoramide (HMPA) followed by treatment with the proper alkyl halide (Scheme 2).

Thiouracil and thiothymine derivatives **6** were obtained by condensation of thiourea in alkaline medium

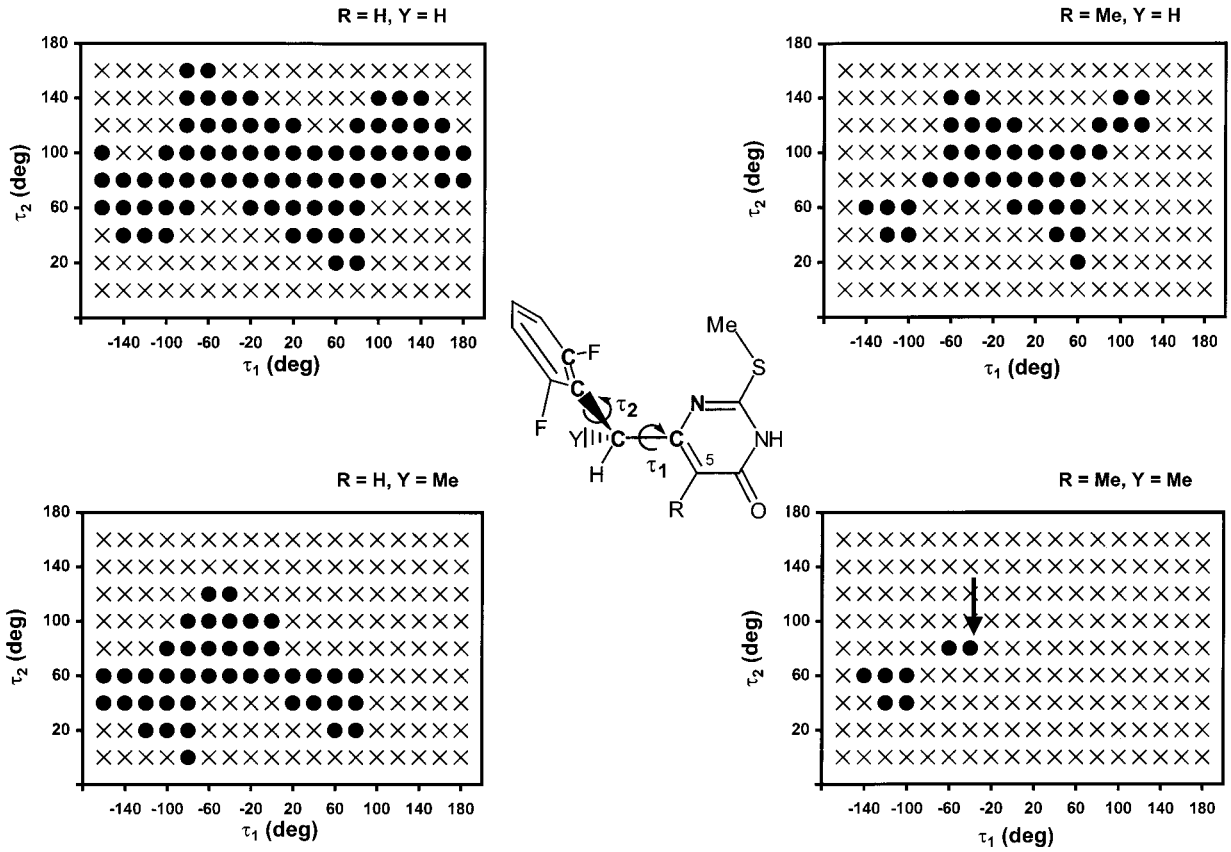

Figure 2. Distribution of the strain energies (E_{strain}) among the conformations of 2,6-difluorobenzyl-*S*-DABO models differing in the presence or absence of a methyl group at the pyrimidine 5-position and the benzylic carbon with *R* configuration. Torsion angles τ_1 and τ_2 are defined in Figure 1. Circle and cross labels denote E_{strain} values within and above 2 kcal/mol, respectively.

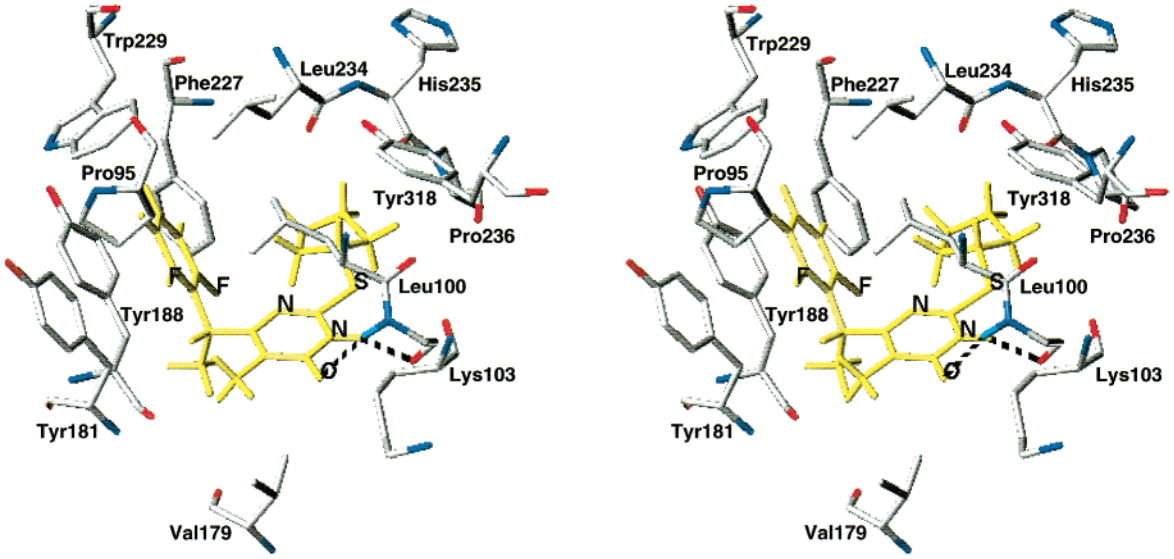

Figure 3. Model of (*R*)-**3w** docked into the RT non-nucleoside binding site. Putative intermolecular hydrogen bonds are highlighted by dashed lines. Only residues within 3.5 Å from the ligand are shown. For sake of clarity, Glu138, Val106, and the side chain of Lys101 are not displayed.

with ethyl 4-aryl-3-oxopentanoates and ethyl 4-aryl-3-oxohexanoates (**5**), respectively. Preparation of the latter *β*-oxoesters was performed by reacting potassium monoethylmalonate or 2-methylmalonate with the proper acylimidazolides in the presence of the magnesium dichloride/triethylamine system.[32] The required 2-arylpropionic or 2-arylbutyric acids **4** were obtained from the related 2-arylacetic acids by lithiation (with LDA in THF and HMPA) and subsequent alkylation.

Chemical and physical data of the newly synthesized derivatives are reported in Tables 1 and 2.

Results and Discussion

The novel *S*-DABOs **3** were evaluated for their cytotoxicity and anti-HIV-1 activity in MT-4 cells (Table 3) in comparison with nevirapine,[9] MKC-442,[15] and six previously reported *S*-DABOs (**2a**−**f**).[32] Selected compounds were assayed against highly purified recombi-

Scheme 1[a]

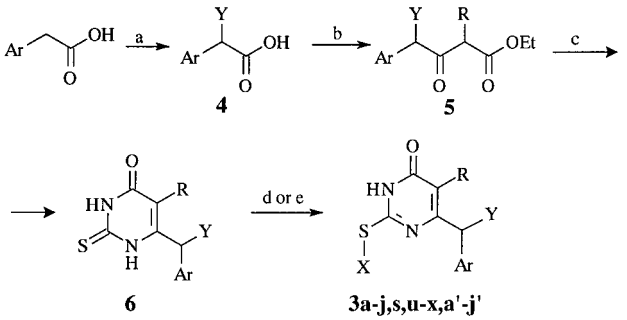

[a] R = H, Me; Y = Me, Et; Ar = phenyl, 1-naphthyl, 2,6-F_2-phenyl, 2,6-Cl_2-phenyl; X = alkyl, cycloalkyl. (a) (1) LDA, THF, and HMPA, 0 °C; (2) YI, H^+. (b) (1) CDI, CH_3CN, room temp; (2) EtOCOCHRCOOK, $(C_2H_5)_3N$, $MgCl_2$, CH_3CN, room temp; (3) 13% HCl. (c) (1) C_2H_5ONa, NH_2CSNH_2, C_2H_5OH, reflux; (2) 2 N HCl. (d) X-halide, K_2CO_3, DMF, room temp. (e) $C_6H_{11}I$, K_2CO_3, DMF, 80 °C.

Scheme 2[a]

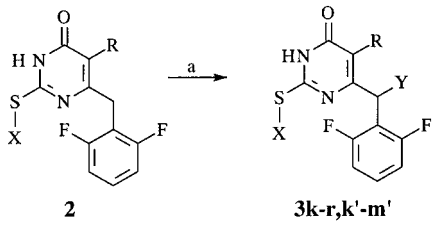

[a] R = H, Me; X = alkyl, cycloalkyl; Y = Me, Et. (a) (1) LDA, THF, and HMPA, 0 °C; (2) alkyl halide, H^+.

nant wild-type HIV-1 RT using homopolymeric template primers. The results, expressed as CC_{50} (cytotoxicity), EC_{50} (anti-HIV-1 activity), SI (selectivity, given by the CC_{50}/EC_{50} ratio), and IC_{50} (RT inhibitory activity) values, are summarized in Table 3.

In the 2,6-difluorobenzylthymine (R = Me) series, methylation of the benzylic carbon improves anti-HIV-1 and RT inhibitory activities (compare **3s**, **3t**, and **3w** vs the α-desmethyl counterparts **2d**, **2e**, and **2f**) together with selectivity. Compound **3w** is the most potent and selective among the newly disclosed *S*-DABOs (CC_{50} > 200 μM, EC_{50} = 6 nM, IC_{50} = 5 nM, and SI > 33 333), inhibiting HIV-1 replication in MT-4 cells more effectively than MKC-442 (by 5-fold), nevirapine (by 50-fold), and its α-desmethyl homologue **2f** (by 13-fold). Assays performed on pure enantiomers of **3w**, obtained by resolution of the racemic mixture by chiral HPLC,[37] showed that configuration is a crucial determinant for activity since (+)-**3w** (CC_{50} > 200 μM, EC_{50} = 2 nM, IC_{50} = 8 nM, and SI > 100 000) is 350 and 125 times more active than (−)-**3w** in the cell-based and enzymatic tests, respectively. All of the 2,6-difluorobenzyluracils are generally less active by 4- to 9-fold than the corresponding thymines (except **3o** and **3t**, which are equipotent). In contrast, uracil and thymine derivatives of type **2** exhibited similar anti-HIV and anti-RT activities [32] (compare **2a**, **2b**, and **2c** with **2d**, **2e**, and **2f**). In other words, methylation of the benzylic carbon enhances activity provided that an additional methyl group is in place at the pyrimidine 5-position, as though the two methyls exerted a sort of synergistic effect on potency. These findings are consistent with our hypothesis of the two methyls restricting the conformational freedom of α-methylthymines to only a few low-energy conformations, including the one bound to RT.

The nature of the 2-alkylthio substituent modulates antiviral RT inhibiting activity. The methylthio is the least performant in both uracil and thymine series probably because the alkylthio side chain must fulfill minimal requirements of lipophilicity. Steric properties of the 2-alkylthio substituent also affect activity as examplified by the 3- and 5-fold drop of activity passing from the *c*-pentylthio derivatives **3w** and **3p** to the corresponding *c*-hexylthio homologues **3x** and **3q**.

When the methyl at the benzylic carbon is replaced by an ethyl, activity is retained or decreases slightly (up to 5-fold passing from **3p** to **3l′**) with the exception of the pairs **3q**, **3m′** and **3h**, **3h′** wherein the α-ethyl derivatives are 3-fold more active. These results suggest that the dimensions of the cavity within the RT hosting the α-substituent would not be compatible with groups larger than ethyl.

Aryl moieties different from the 2,6-difluorophenyl (phenyl, 1-naphthyl, 2,6-dichlorophenyl) are generally detrimental to activity, the only exception being the 1-naphthyl derivative **3g**, which is slightly more active than the corresponding 2,6-difluorophenyl derivative **3p**. The above findings are in accordance with a favorable electronic effect exerted by the 2,6-fluorines on a putative charge-transfer interaction between the aromatic moieties of the inhibitor and Tyr188.

The doses required to reduce HIV-1 p24 antigen levels by 90%, 99%, and 99.9% were determined for a few representative 2,6-difluorobenzyl-*S*-DABOs **2** and **3** in comparison with MKC-442 (Table 4). In these secondary tests, compound **3w** confirms its highest activity (EC_{90} = 6 nM, EC_{99} = 15 nM, $EC_{99.9}$ = 33 nM).

Three compounds (**2f**, **3r**, and **3t**) among those most active were submitted to a preliminary test against the Y181C HIV-1 mutant strain using nevirapine and efavirenz[38] as reference drugs. As shown by preliminary data on Y181C inhibition (Table 5), the presence of substituents at both the C-5 pyrimidine ring and the CH_2 linker plays an important role. In fact, the thymine derivative **2f**, which does not bear substituents at the methylene linker, is less potent than the linker-substituted thymine derivative **3t**. However, the nature and length of the *S*-substituent play a determinant role for inhibitory potency against Y181C mutant as proved by comparing the potent *sec*-butylthio derivative **3t** with the scarcely active methylthio counterpart **3r**.

Studies are in progress to confirm that, having as untouchable basic structure the 6-[1-(2,6-difluorophenyl)ethyl]-5-methyl-3,4-dihydropyrimidin-4-one moiety, the activity of F_2-*S*-DABOs against Y181C mutant strain could be properly modulated by introducing appropriate alkyl (or cycloalkyl)thio substituents in the C-2 position.

Conclusions

Conformationally restricted *S*-DABOs **3**, bearing a methyl or ethyl group on the benzylic carbon, were designed as novel NNRTIs using computational methods. Biological evaluation of the newly synthesized compounds identified the 2,6-difluorobenzyl-α-methylthymine derivatives as those most active in reducing

Table 1. Physical and Chemical Data of Compounds **3**

compd	Ar	R	Y	X	mp, °C	recryst solvent	synth scheme[a]	% yield	formula[b]
3a	Ph	H	Me	*i*-Pr	118−119	*n*-hexane	1	88	$C_{15}H_{18}N_2Os$
3b	Ph	H	Me	*s*-Bu	97−98	*n*-hexane	1	69	$C_{16}H_{20}N_2OS$
3c	Ph	H	Me	cyclopentyl	95−96	*n*-hexane	1	74	$C_{17}H_{20}N_2OS$
3d	Ph	H	Me	cyclohexyl	142−143	*n*-hexane	1	62	$C_{18}H_{22}N_2OS$
3e	1-naphthyl	H	Me	*i*-Pr	161−163	*n*-hexane/cyclohex	1	70	$C_{19}H_{20}N_2OS$
3f	1-naphthyl	H	Me	cyclopentyl	oil		1	58	$C_{21}H_{22}N_2OS$
3g	1-naphthyl	H	Me	cyclohexyl	177−178	*n*-hexane	1	46	$C_{22}H_{24}N_2OS$
3h	2,6-Cl_2-Ph	H	Me	*i*-Pr	168−170	diethyl ether	1	69	$C_{15}H_{16}Cl_2N_2OS$
3i	2,6-Cl_2-Ph	H	Me	cyclopentyl	181−182	cyclohexane	1	63	$C_{17}H_{18}Cl_2N_2OS$
3j	2,6-Cl_2-Ph	H	Me	cyclohexyl	211−212	benzene/cyclohex	1	49	$C_{18}H_{20}Cl_2N_2OS$
3k	2,6-F_2-Ph	H	Me	Me	179−180	benzene	2	41	$C_{13}H_{12}F_2N_2OS$
3l	2,6-F_2-Ph	H	Me	*i*-Pr	155−156	cyclohexane	2	60	$C_{15}H_{16}F_2N_2OS$
3m	2,6-F_2-Ph	H	Me	*n*-Bu	149−150	cyclohexane	2	56	$C_{16}H_{18}F_2N_2OS$
3n	2,6-F_2-Ph	H	Me	*i*-Bu	159−160	cyclohexane	2	54	$C_{16}H_{18}F_2N_2OS$
3o	2,6-F_2-Ph	H	Me	*s*-Bu	133−134	*n*-hexane	2	55	$C_{16}H_{18}F_2N_2OS$
3p	2,6-F_2-Ph	H	Me	cyclopentyl	165.5−166.5	cyclohexane	2	54	$C_{17}H_{18}F_2N_2OS$
3q	2,6-F_2-Ph	H	Me	cyclohexyl	206−207	benzene	2	32	$C_{18}H_{20}F_2N_2OS$
3r	2,6-F_2-Ph	Me	Me	Me	202−203	benzene/cyclohex	2	49	$C_{14}H_{14}F_2N_2OS$
3s	2,6-F_2-Ph	Me	Me	*i*-Pr	177−178	*n*-hexane/cyclohex	1	69	$C_{16}H_{18}F_2N_2OS$
3t	2,6-F_2-Ph	Me	Me	*s*-Bu	135−136	cyclohexane	2	55	$C_{17}H_{20}F_2N_2OS$
3u	2,6-F_2-Ph	Me	Me	*n*-Bu	122−123	*n*-hexane	1	58	$C_{17}H_{20}F_2N_2OS$
3v	2,6-F_2-Ph	Me	Me	*i*-Bu	152−153	cyclohexane	1	62	$C_{17}H_{20}F_2N_2OS$
3w	2,6-F_2-Ph	Me	Me	cyclopentyl	196−197	cyclohexane	1	60	$C_{18}H_{20}F_2N_2OS$
3x	2,6-F_2-Ph	Me	Me	cyclohexyl	208−209	*n*-hexane/cyclohex	1	48	$C_{19}H_{22}F_2N_2OS$
3a′	Ph	H	Et	*i*-Pr	144−145	cyclohexane	1	82	$C_{16}H_{20}N_2OS$
3b′	Ph	H	Et	*s*-Bu	138−139	cyclohexane	1	62	$C_{17}H_{22}N_2OS$
3c′	Ph	H	Et	cyclopentyl	168−169	cyclohexane	1	75	$C_{18}H_{22}N_2OS$
3d′	Ph	H	Et	cyclohexyl	175.5−176.5	cyclohexane	1	58	$C_{19}H_{24}N_2OS$
3e′	1-naphthyl	H	Et	*i*-Pr	163−164	cyclohexane	1	67	$C_{20}H_{22}N_2OS$
3f′	1-naphthyl	H	Et	cyclopentyl	oil		1	52	$C_{22}H_{24}N_2OS$
3 g′	1-naphthyl	H	Et	cyclohexyl	126−127	*n*-hexane	1	44	$C_{23}H_{26}N_2OS$
3h′	2,6-F_2-Ph	H	Et	*i*-Pr	166−168	diethyl ether	1	64	$C_{16}H_{18}Cl_2N_2OS$
3i′	2,6-F_2-Ph	H	Et	cyclopentyl	168−169	diethyl ether	1	58	$C_{18}H_{20}Cl_2N_2OS$
3j′	2,6-F_2-Ph	H	Et	cyclohexyl	198−199	cyclohexane	1	62	$C_{19}H_{22}Cl_2N_2OS$
3k′	2,6-F_2-Ph	H	Et	*i*-Pr	149−150	cyclohexane	2	58	$C_{16}H_{18}F_2N_2OS$
3l′	2,6-F_2-Ph	H	Et	cyclopentyl	141−143	cyclohexane	2	59	$C_{18}H_{20}F_2N_2OS$
3m′	2,6-F_2-Ph	H	Et	cyclohexyl	154−155	cyclohexane	2	54	$C_{19}H_{22}F_2N_2OS$

[a] See Schemes 1 and 2. [b] All compounds were analyzed for C, H, N, S and, when required, Cl and F. Analytical results were within ±0.4% of the theoretical values.

Table 2. Physical and Chemical Data of Compounds **4**−**6**

compd	Ar	R	Y	mp, °C	recryst solvent	synth scheme[a]	% yield	formula[b]
4a	1-naphthyl		Me	142−143	cyclohexane	a	86	$C_{13}H_{12}O_2$
4b	2,6-Cl_2-Ph		Me	124−125	cyclohexane	a	68	$C_9H_8Cl_2O_2$
4c	2,6-F_2-Ph		Me	oil		a	65	$C_9H_8F_2O_2$
4d	1-naphthyl		Et	86−87	*n*-hexane	a	100	$C_{14}H_{14}O_2$
4e	2,6-Cl_2-Ph		Et	131−132	cyclohexane	a	59	$C_{10}H_{10}Cl_2O_2$
4f	2,6-F_2-Ph		Et	oil		a	47	$C_{10}H_{10}F_2O_2$
5a	Ph	H	Me	oil		b	88	$C_{13}H_{16}O_3$
5b	1-naphthyl	H	Me	oil		b	98	$C_{17}H_{18}O_3$
5c	2,6-Cl_2-Ph	H	Me	oil		b	86	$C_{13}H_{14}Cl_2O_3$
5d	2,6-F_2-Ph	H	Me	oil		b	90	$C_{13}H_{14}F_2O_3$
5e	2,6-F_2-Ph	Me	Me	oil		b	74	$C_{14}H_{16}F_2O_3$
5f	Ph	H	Et	oil		b	94	$C_{14}H_{18}O_3$
5g	1-naphthyl	H	Et	oil		b	94	$C_{18}H_{20}O_3$
5h	2,6-Cl_2-Ph	H	Et	oil		b	89	$C_{14}H_{16}Cl_2O_3$
5i	2,6-F_2-Ph	H	Et	oil		b	87	$C_{14}H_{16}F_2O_3$
6a	Ph	H	Me	205−206	ethanol	c	64	$C_{12}H_{12}N_2OS$
6b	1-naphthyl	H	Me	229−230	acetonitrile	c	41	$C_{16}H_{14}N_2OS$
6c	2,6-Cl_2-Ph	H	Me	252−253	ethanol	c	54	$C_{12}H_{10}Cl_2N_2OS$
6d	2,6-F_2-Ph	H	Me	267−268	ethanol	c	59	$C_{12}H_{10}F_2N_2OS$
6e	2,6-F_2-Ph	Me	Me	267−269	acetonitrile	c	40	$C_{13}H_{12}F_2N_2OS$
6f	Ph	H	Et	242−243	ethanol	c	48	$C_{13}H_{14}N_2OS$
6g	1-naphthyl	H	Et	244−246	ethanol/water	c	42	$C_{17}H_{16}N_2OS$
6h	2,6-Cl_2-Ph	H	Et	222−223	ethanol	c	61	$C_{13}H_{12}Cl_2N_2OS$
6i	2,6-F_2-Ph	H	Et	202−203	diethyl ether	c	42	$C_{13}H_{12}F_2N_2OS$

[a] See schemes 1. [b] All compounds were analyzed for C, H, and, when required, N, S, Cl, and F. Analytical results were within ±0.4% of the theoretical values.

HIV-1-induced cytopathicity in MT-4 cells and inhibiting wild-type RT, thus confirming the rationale leading to their synthesis. The significant improvement of potency associated with two methyl groups, one at the benzylic carbon and the other at the pyrimidine 5-position, was related to an intramolecular steric effect; in the *R* enantiomer the conformational space is restricted to a few low-energy conformations including the one recog-

Table 3. Cytotoxicity and Anti-HIV-1 Activity of Compounds **3**[a]

compd	Ar	R	Y	X	[μM] CC_{50}[b]	[μM] EC_{50}[c]	[μM] IC_{50}[d]	SI[e]
3a	Ph	H	Me	*i*-Pr	>200[f]	0.9	2.3	>222
3b	Ph	H	Me	*s*-Bu	200	0.23	ND[g]	870
3c	Ph	H	Me	cyclopentyl	159	0.6	2.1	333
3d	Ph	H	Me	cyclohexyl	149	0.6	ND	248
3e	1-naphthyl	H	Me	*i*-Pr	119	1.1	5.8	108
3f	1-naphthyl	H	Me	cyclopentyl	93	0.5	0.4	186
3g	1-naphthyl	H	Me	cyclohexyl	45	0.14	2.6	321.4
3h	2,6-Cl_2-Ph	H	Me	*i*-Pr	117	1.2	ND	97.5
3i	2,6-Cl_2-Ph	H	Me	cyclopentyl	78.3	1.0	ND	78.3
3j	2,6-Cl_2-Ph	H	Me	cyclohexyl	>200	2.9	ND	>69
3k	2,6-F_2-Ph	H	Me	Me	20.8	0.18	0.2	115
3l	2,6-F_2-Ph	H	Me	*i*-Pr	167	0.05	ND	3340
3m	2,6-F_2-Ph	H	Me	*n*-Bu	>200	0.07	ND	2857
3n	2,6-F_2-Ph	H	Me	*i*-Bu	>200	0.05	ND	>4000
3o	2,6-F_2-Ph	H	Me	*s*-Bu	>200	0.03	ND	>6666
3p	2,6-F_2-Ph	H	Me	cyclopentyl	>200	0.03	0.05	>6666
3q	2,6-F_2-Ph	H	Me	cyclohexyl	>200	0.16	ND	>1250
3r	2,6-F_2-Ph	Me	Me	Me	>200	0.04	0.02	>5000
3s	2,6-F_2-Ph	Me	Me	*i*-Pr	200	0.007	0.019	>28570
3t	2,6-F_2-Ph	Me	Me	*s*-Bu	>200	0.03	0.02	6666
3u	2,6-F_2-Ph	Me	Me	*n*-Bu	112	0.008	ND	14000
3v	2,6-F_2-Ph	Me	Me	*i*-Bu	>200	0.01	ND	>20000
3w	2,6-F_2-Ph	Me	Me	cyclopentyl	>200	0.006	0.005	>33333
[+]-**3w**[h]	2,6-F_2-Ph	Me	Me	cyclopentyl	>200	0.002	0.008	>100000
[−]-**3w**[h]	2,6-F_2-Ph	Me	Me	cyclopentyl	200	0.07	1.0	>286
3x	2,6-F_2-Ph	Me	Me	cyclohexyl	>200	0.018	ND	>11111
3a′	Ph	H	Et	*i*-Pr	>200	0.8	2.3	250
3b′	Ph	H	Et	*s*-Bu	>200	0.4	ND	>500
3c′	Ph	H	Et	cyclopentyl	50	1.0	>10	>200
3d′	Ph	H	Et	cyclohexyl	51	1.3	3.7	>154
3e′	1-naphthyl	H	Et	*i*-Pr	16.9	1.5	0.8	33.3
3f′	1-naphthyl	H	Et	cyclopentyl	>200	3.0	ND	17
3g′	1-naphthyl	H	Et	cyclohexyl	23.4	0.18	1.4	94
3h′	2,6-Cl_2-Ph	H	Et	*i*-Pr	>200	0.4	ND	>500
3i′	2,6-Cl_2-Ph	H	Et	cyclopentyl	70	1.0	ND	23.4
3j′	2,6-Cl_2-Ph	H	Et	cyclohexyl	200	3.6	ND	>55.5
3k′	2,6-F_2-Ph	H	Et	*i*-Pr	130	0.08	ND	875
3l′	2,6-F_2-Ph	H	Et	cyclopentyl	>200	0.15	ND	1333
3m′	2,6-F_2-Ph	H	Et	cyclohexyl	>200	0.05	ND	2600
2a[i]	2,6-F_2-Ph	H		*i*-Pr	>200	0.05	0.05	>4000
2b	2,6-F_2-Ph	H		*s*-Bu	>200	0.04	0.05	>5000
2c	2,6-F_2-Ph	H		cyclopentyl	>200	0.08	0.08	>2500
2d	2,6-F_2-Ph	Me		*i*-Pr	>200	0.05	0.05	>4000
2e	2,6-F_2-Ph	Me		*s*-Bu	200	0.05	0.05	>4000
2f	2,6-F_2-Ph	Me		cyclopentyl	>200	0.08	0.08	>2500
MKC-422					200	0.03	0.04	6666
nevirapine					>200	0.3	0.3	>666

[a] Data represent mean values of at least two separate experiments. [b] Compound dose required to reduce the viability of mock-infected cells by 50%, as detemined by the MTT method. [c] Compound dose required to achieve 50% protection of MT-4 cells from HIV-1-induced cytopathogenicity, as determined by the MTT method. [d] Compound dose required to inhibit the HIV-1 rRT activity by 50%. [e] Selectivity index, CC_{50}/EC_{50} ratio. [f] Higher concentrations could not be achieved for crystallization of compounds in the culture medium [g] Not determined. [h] [+] and [−] are referred to CDC values recorded at 244 nm (ref 37). [i] Reference 32.

Table 4. Anti-HIV-1 Activity of F_2-*S*-DABOs **2** and **3** as Determined by Reduction of p24 Levels

compd	R	Y	X	[μM] EC_{90}[a]	[μM] EC_{99}[a]	[μM] $EC_{99.9}$[a]
2a	H		*i*-Pr	0.042	0.083	0.190
2c	H		cyclopentyl	0.080	0.150	0.300
2d	Me		*i*-Pr	0.026	0.065	0.150
2f	Me		cyclopentyl	0.040	0.075	0.150
3l	H	Me	*i*-Pr	0.042	0.083	0.190
3p	H	Me	cyclopentyl	0.015	0.035	0.090
3w	Me	Me	cyclopentyl	0.006	0.015	0.033
3k′	H	Et	*i*-Pr	0.015	0.035	0.090
3l′	H	Et	cyclopentyl	0.080	0.150	0.300
MKC-442				0.014	0.041	0.082

[a] Compound dose required to reduce p24 antigen levels by 90% (EC_{90}), 99% (EC_{99}), and 99.9% ($EC_{99.9}$).

Table 5. Activity of Selected F_2-*S*-DABOs **2** and **3** against Y181C HIV-1 Mutant Strain

compd	R	Y	X	EC_{50}, μM[a] WT_{IIIB}	EC_{50}, μM[a] Y181C	(Y181C/WT_{IIIB})[b]
2f	Me		cyclopentyl	0.04	1.2	(30)
3r	Me	Me	Me	0.037	≥10	(≥270)
3t	Me	Me	*s*-Bu	0.02	0.3	(15)
nevirapine				0.37	>30	(>81)
efavirenz				0.004	0.025	(6)

[a] Compound dose required to achieve 50% protection of MT-4 cells for wild-type and Y181C HIV-1-induced cytopathogenicity, as determined by the MTT method. [b] Fold resistance.

nized by RT. Compound (+)-**3w**, significantly more active and less cytotoxic than the corresponding enantiomer (−)-**3w**, exhibited the highest activity and selectivity among the so-far reported *S*-DABOs (CC_{50} > 200 μM, EC_{50} = 2 nM, IC_{50} = 8 nM, SI > 100 000) under conditions wherein the MKC-442 was less active and selective (CC_{50} > 200 μM, EC_{50} = 30 nM, IC_{50} = 40 nM,

SI > 6666). These results make compound (+)-**3w** an interesting candidate for further biological and pharmacological studies aimed at evaluating its effectiveness as an anti-AIDS agent.

Experimental Section

Chemistry. Melting points were determined on a Büchi 530 melting point apparatus and are uncorrected. Infrared (IR) spectra (KBr) were recorded on a Perkin-Elmer 310 instrument. ^{1}H NMR spectra were recorded at 200 MHz on a Bruker AC 200 spectrometer; chemical shifts are reported in δ (ppm) units relative to the internal reference tetramethylsilane (Me_4-Si). All compounds were routinely checked by TLC and ^{1}H NMR. TLC was performed on aluminum-backed silica gel plates (Merck DC-Alufolien Kieselgel 60 F_{254}) with spots visualized by UV light. All solvents were reagent grade and, when necessary, were purified and dried by standards methods. The concentrations of solutions after reactions and extractions involved the use of a rotary evaporator operating at a reduced pressure of ca. 20 Torr. Organic solutions were dried over anhydrous sodium sulfate. Analytical results are within ±0.40% of the theoretical values. Arylacetic acids, *N*,*N*′-carbonyldiimidazole, iodomethane, 2-iodopropane, 1-iodo-2-methylpropane, 2-iodobutane, 1-iodobutane, cyclopentyl bromide, and cyclohexyl iodide were purchased from Aldrich Chimica, Milan (Italy), or Lancaster Synthesis GmbH, Milan (Italy).

Syntheses. The specific examples presented below illustrate general synthetic methods. As a rule, samples prepared for physical (Tables 1 and 2) and biological studies (Tables 3−5) were dried in high vacuum over P_2O_5 for 20 h at temperatures ranging from 25 to 110 °C, depending on the sample melting point.

Synthesis of 4. Example: 2-(2,6-Difluorophenyl)propionic Acid (4c). 2-(2,6-Difluorophenyl)acetic acid (3.00 g, 17.43 mmol) was added portionwise to a cooled (0 °C) 2.0 M solution of LDA in heptane/THF/ethylbenzene (26.5 mL, 52.29 mmol), and then HMPA (4.57 mL, 26.14 mmol) and THF (10 mL) were added to the mixture. The resulting solution was stirred at room temperature for 30 min, then it was recooled (0 °C), treated with methyl iodide (3.72 g, 1.63 mL, 26.14 mmol), and stirred at room temperature for 5 min. After being stirred, the clear solution was poured into cold water (200 mL) and 2 N HCl (20 mL) and extracted with ethyl acetate (3 × 50 mL). The organic layers were collected, washed with brine (100 mL), dried, and evaporated to furnish a residue that was purified by column chromatography (silica gel, ethyl acetate/chloroform 1/1). ^{1}H NMR ($CDCl_3$): δ 1.49−1.52 (d, 3H, CH_3), 4.07−4.18 (q, 1H, CH), 6.82−6.90 (m, 2H, C-3,5 Ar-H), 7.15−7.24 (m, 1H, C-4 Ar-H), 7.95 (s, 1H, OH exchangeable with D_2O). IR: 3060, 1700 cm^{-1}. Anal. C, H, F.

Synthesis of 5. Example: Ethyl 4-(1-Naphthyl)-3-oxohexanoate (5g). Triethylamine (11.6 mL, 83.2 mmol) and magnesium dichloride (6.33 g, 66.5 mmol) were added to a stirred suspension of potassium ethylmalonate (9.51 g, 55.8 mmol) in dry acetonitrile (100 mL), and stirring was continued at room temperature for 2 h. Then, a solution of the 2-(1-naphthyl)butanoic imidazolide in the same solvent (50 mL), prepared 15 min before by reaction between 2-(1-naphthyl)-butanoic acid (**4d**) (5.70 g, 26.6 mmol) and *N*,*N*′-carbonyldiimidazole (5.17 g, 32.0 mmol) in acetonitrile (50 mL), was added. The reaction mixture was stirred overnight at room temperature and then was completed by heating at reflux for 2 h. After the mixture was cooled, 13% HCl (100 mL) was cautiously added while the temperature was kept below 25 °C, and the resulting clear mixture was stirred for a further 15 min. The organic layer was separated and evaporated, and the residue was treated with ethyl acetate (100 mL). The aqueous layer was extracted with ethyl acetate (2 × 50 mL), and the organic phases were collected, washed with sodium hydrogen carbonate saturated solution (2 × 100 mL) and brine (100 mL), dried, and concentrated to give pure **5g** (7.08 g). ^{1}H NMR ($CDCl_3$): δ 0.85−0.93 (t, 3H, $CHCH_2CH_3$), 1.10−1.17 (t, 3H, OCH_2CH_3), 1.79−1.97 (m, 1H, $CHCH_2CH_3$), 2.19−2.36 (m, 1H, $CHCH_2CH_3$), 3.24−3.27 (d, 2H, $COCH_2CO$), 3.97−4.07 (q, 2H, OCH_2CH_3), 4.43−4.50 (t, 1H, $CHCH_2CH_3$), 7.24−7.34 (m, 1H, C-2 naphthyl-H), 7.39−7.58 (m, 3H, C-3,6,7 naphthyl-H), 7.76−7.89 (m, 2H, C-4,8 naphthyl-H), 8.05−8.09 (m, 1H, C-5 naphthyl-H). IR: 1725, 1695 cm^{-1}. Anal. C, H.

Synthesis of 6. Example: 6-[1-(2,6-Dichlorophenyl)-ethyl]-3,4-dihydro-2-thioxopyrimidin-4(3*H*)-one (6c). Sodium metal (0.60 g, 26.2 mmol) was dissolved in 50 mL of absolute ethanol, and thiourea (1.39 g, 18.2 mmol) and ethyl 4-(2,6-dichlorophenyl)-3-oxopentanoate (**5c**) (3.53 g, 13.1 mmol) were added to the clear solution. The mixture was heated at reflux for 5 h. After the mixture was cooled, the solvent was distilled in vacuo at 40−50 °C until dry and the residue was dissolved in a little water (20 mL) and made acidic with 2 N HCl. The resulting precipitate was filtered under reduced pressure, washed with diethyl ether, and vacuum-dried at 80 °C for 12 h to give 2.2 g of **6c** as a pure solid. ^{1}H NMR (DMSO-d_6): δ 1.46−1.50 (d, 2H, CH_3), 4.54−4.57 (q, 1H, CH-Ar), 5.71 (s, 1H, C-5 H), 7.28−7.35 (m, 1H, C-4 Ar-H), 7.42−7.47 (m, 2H, C-3,5 Ar-H), 12.17 (s, 1H, NH exchanged with D_2O), 12.36 (s, 1H, NH exchanged with D_2O). IR: 3100, 1630 cm^{-1}. Anal. C, H, Cl, N, S.

Synthesis of 3 from 6. Example 1: 2-Cyclopentylthio-3,4-dihydro-6-(1-phenyl)ethylpyrimidin-4(3*H*)-one (3c). A mixture of 3,4-dihydro-6-(1-phenylethyl)-2-thioxopyrimidin-4(3*H*)-one (**6a**) (0.15 g, 0.65 mmol), cyclopentyl bromide (0.11 g, 0.08 mL, 0.71 mmol), and potassium carbonate (0.09 g, 0.65 mmol) in 1 mL of anhydrous DMF was stirred at room temperature for 24 h. After treatment with cold water (200 mL), the solution was extracted with ethyl acetate (3 × 50 mL). The organic layers were collected, washed with brine (3 × 50 mL), dried, and evaporated to furnish crude **3c**, which was purified by chromatography on silica gel column (eluent: *n*-hexane/ethyl acetate/methanol 12/3/1). ^{1}H NMR ($CDCl_3$): δ 1.56−1.59 (d, 3H, $CHCH_3$), 1.79−1.71 (m, 6H, C-2eq,5eq, C-3, C-4 cyclopentane-H overlapped signal), 2.07−2.09 (m, 2H, C-2ax,5ax cyclopentane-H), 3.82−3.93 (q, 1H, $CHCH_3$), 3.93−4.02 (m, 1H, SCH overlapped signal), 6.02 (s, 1H, C-5 H), 7.25−7.27 (m, 5H, Ph), 13.00 (broad s, 1H, NH exchanged with D_2O). IR: 2950, 1630 cm^{-1}. Anal. C, H, N, S.

Synthesis of 3 from 6. Example 2: 2-Cyclohexylthio-3,4-dihydro-6-[1-(1-naphthyl)propyl]pyrimidin-4(3*H*)-one (3g′). A mixture of 3,4-dihydro-6-[1-(1-naphthylpropyl)]-2-thioxopyrimidin-4(3*H*)-one (**6g**) (0.50 g, 1.69 mmol), cyclohexyl iodide (0.39 g, 0.24 mL, 1.86 mmol), and potassium carbonate (0.23 g, 1.69 mmol) in 2 mL of anhydrous DMF was heated at 80 °C for 15 h. After cooling, the reaction mixture was treated with cold water (100 mL) and extracted with ethyl acetate (3 × 50 mL). The organic layers were collected, washed with brine (3 × 50 mL), dried, and evaporated to furnish crude **3g′**, which was purified by chromatography on a silica gel column (eluent: *n*-hexane/ethyl acetate/methanol, 12/3/1). ^{1}H NMR ($CDCl_3$): δ 0.93−1.00 (t, 3H, $CHCH_2CH_3$), 1.28−1.63 (m, 6H, C-3,4,5 cyclohexane-H), 1.63−1.70 (m, 2H, C-2eq,6eq cyclohexane-H overlapped signal), 1.91−1.96 (m, 2H, C-2ax,6ax cyclohexane-H), 2.06−2.24 (m, 1H, $CHCH_2CH_3$), 2.24−2.34 (m, 1H, $CHCH_2CH_3$), 3.72−3.76 (m, 1H, SCH), 4.39−4.46 (t, 1H, $CHCH_2CH_3$), 6.11 (s, 1H, C-5 H), 7.42−7.50 (m, 4H, C-2,3,6,7 naphthyl-H), 7.69−7.73 (m, 1H, C-4 naphthyl-H), 7.79−7.84 (m, 1H, C-8 naphthyl-H), 8.07−8.11 (m, 1H, C-5 naphthyl-H), 12.59 (s, 1H, NH exchanged with D_2O). IR: 2900, 1645 cm^{-1}. Anal. C, H, N, S.

Synthesis of 3 from 2. Example: 2-Cyclopentylthio-6-[1-(2,6-difluorophenyl)propyl]-3,4-dihydropyrimidin-4(3*H*)-one (3l′). 2-Cyclopentylthio-6-(2,6-difluorobenzyl)-3,4-dihydropyrimidin-4(3*H*)-one (**2c**)[32] (0.70 g, 2.08 mmol) was added portionwise to a cooled (0 °C) 2.0 M solution of LDA in heptane/THF/ethylbenzene (6.3 mL, 12.48 mmol), and then HMPA (0.55 mL, 3.12 mmol) and THF (10 mL) were added to the mixture. The resulting solution was stirred at room temperature for 30 min, then it was recooled (0 °C), rapidly treated with ethyl iodide (0.48 g, 0.25 mL, 3.12 mmol), and stirred at room temperature overnight. After the mixture

was stirred, the clear solution was poured into cold water (200 mL) and 2 N HCl (20 mL) and extracted with ethyl acetate (3 × 50 mL). The organic layers were collected, washed with brine (100 mL), dried, and evaporated to furnish a residue that was purified by column chromatography (silica gel, ethyl acetate/chloroform 1/1). ^{1}H NMR ($CDCl_3$): δ 0.87−0.94 (t, 3H, $CHCH_2CH_3$), 1.25−1.84 (m, 8H, C-2eq,6eq,3,4,5 cyclohexane-H), 1.95−2.10 (m, 3H, C-2ax,6ax cyclohexane-H and $CHCH_2$-CH_3), 2.16−2.26 (m, 1H, $CHCH_2CH_3$), 3.63−3.67 (m, 1H, SCH), 4.06−4.14 (dd, 1H, $CHCH_2CH_3$), 6.13 (s, 1H, C-5 H), 6.77−6.85 (t, 2H, C-3,5 Ar-H), 7.11−7.18 (m, 1H, C-4 Ar-H), 12.80 (s, 1H, NH exchanged with D_2O). IR: 2800, 1645 cm^{-1}. Anal. C, H, F, N, S.

Antiviral Assay Procedures. Compounds. Compounds were solubilized in DMSO at 200 mM and then diluted into a culture medium.

Cells and Viruses. MT-4, C8166, H9/III$_B$, and CEM cells were grown at 37 °C in a 5% CO_2 atmosphere in RPMI 1640 medium, supplemented with 10% fetal calf serum (FCS), 100 IU/mL penicillin G, and 100 μg/mL streptomycin. Cell cultures were checked periodically for the absence of mycoplasma contamination with a MycoTect Kit (Gibco). Human immunodeficiency viruses type-1 (HIV-1, III$_B$ strain) and type-2 (HIV-2 ROD strain, kindly provided by Dr. L. Montagnier, Paris) were obtained from supernatants of persistently infected H9/III$_B$ and CEM cells, respectively. HIV-1 and HIV-2 stock solutions had titers of 4.5×10^6 and 1.4×10^5 50% cell culture infectious dose ($CCID_{50}$)/mL, respectively.

HIV Titration. Titration of HIV was performed in C8166 cells by the standard limiting dilution method (dilution 1:2, four replica wells/dilution) in 96-well plates. The infectious virus titer was determined by light-microscope scoring of cytopathicity after 4 days of incubation, and the virus titers were expressed as $CCID_{50}$/mL.

Anti-HIV Assays. Activity of the compounds against HIV-1 and HIV-2 multiplication in acutely infected cells was based on the inhibition of virus-induced cytopathicity in MT-4 and C8166 cells, respectively. Briefly, 50 μL of culture medium containing 1×10^4 cells was added to each well of flat-bottom microtiter trays containing 50 μL of culture medium with or without various concentrations of the test compounds. Then 20 μL of an HIV suspension containing 100 (HIV-1) or 1000 (HIV-2) $CCID_{50}$ was added. After a 4-day incubation (5 days for HIV-2) at 37 °C, the number of viable cells was determined by the 3-(4,5-dimethylthiazol-1-yl)-2,5-diphenyltetrazolium bromide (MTT) method.[39] Cytotoxicity of the compounds was evaluated in parallel with their antiviral activity. It was based on the viability of mock-infected cells, as monitored by the MTT method.

RT Assays. Assays were performed as previously described.[32]

Briefly, purified rRT was assayed for its RNA-dependent polymerase-associated activity in a 50 μL volume containing 50 mM Tris-HCl (pH 7.8), 80 mM KCl, 6 mM $MgCl_2$, 1 mM DTT, 0.1 mg mL^{-1} BSA, 0.5 OD_{260} unit mL^{-1} template/primer [poly(rC)-oligo(dG)$_{12-18}$], and 10 mM [^{3}H]-dGTP (1 Ci mmol^{-1}). After incubation for 30 min at 37 °C, the samples were spotted on glass fiber filters (Whatman GF/A) and the acid-insoluble radioactivity was determined.

Computational Studies. Computations were performed using the software packages Sybyl[40] and Amber[35,36] running on a Silicon Graphics R10000 workstation. Models of *S*-DABOs were available from previous studies,[32] directly or after modifications according to the standard parameters of the molecular mechanics Tripos force field.[41] In each structure the methyl group of the 2-methylthio side chain and the pyrimidine N1 were oriented in a syn disposition. Geometry optimizations were realized with the Sybyl/Maximin2 minimizer selecting the BFGS (Broyden, Fletcher, Goldfarb, and Shanno) algorithm[42] and a root-mean-square gradient of the forces acting on each atom of 0.05 kcal mol^{-1} Å^{-1} as the convergence criterion. Conformational analyses on the *S*-DABOs in Figure 2 were carried out using the Sybyl/Gridsearch routine. The torsion angles τ_1 and τ_2 (defined in Figure 2) were systematically varied through 20° steps: τ_1 within the 0−340° range and τ_2 within the 0−160° range owing to the equivalence of the 2 and 6 positions of the 2,6-difluorophenyl ring. Each of the generated conformations was energy-minimized without perturbing the scanned torsion angles for a maximum of 15 iterations. The scatter plots in Figure 2 were obtained by calculating the strain energy (E_{strain}) of each conformation as the difference in energy with respect to the global minimum conformation.

The structure of the non-nucleoside binding site (NNBS) of RT was taken from the 2.5 Å resolution of the HIV-1 RT/TNK-651 complex[15] filed in the Brookhaven Protein Data Bank[43] with the entry code 1RT2. The NNBS consisted of a set of 68 amino acids located within 15 Å from the non-hydrogen atoms of the bound inhibitor. Water molecules were removed. Hydrogens were added to the unfilled valences of the protein. Lys, Asp, and Glu side chains were modeled in their ionized forms. The tautomeric states of His residues were assigned by visual inspection. The starting geometry of the NNBS/(*R*)-**3w** complex was modeled on the reported NNBS/**2f** complex.[44] The NNBS extracted from RT/TNK-651 was first aligned on the NNBS/**2f** complex about the backbone atoms and then filled with (*R*)-**3w** obtained by mutation of **2f**.

Energy minimizations (EM) and molecular dynamics (MD) calculations were based on the all-atom Cornell et al. force field[45] available within the Amber package, which was modified to include additional parameters for (*R*)-**3w**. Most of these parameters were either adapted by analogy from others included in the Amber force field or derived from the MM2 force field.[46] Parameters related to the bond distances, bond angles, and torsion angles involving the sulfur atom in the ligand were taken from a parametrization of sulfur-containing compounds.[47,48] Partial atomic charges for the ligand was calculated with the semiempirical quantum mechanics method AM1,[49] available in the Mopac program.[50]

The geometry of the NNBS/(*R*)-**3w** complex was preliminarly optimized by energy minimization with the Sander/Amber module (50 000 steps; distance-dependent dielectric function of $\epsilon = 4r$), applying an energy penalty force constant of 5 kcal/mol to the protein backbone atoms. The geometry-optimized structures were then used as the starting point for subsequent 500 ps MD simulation, during which the protein backbone atoms were constrained as done in the previous step. A time step of 1 fs and a nonbonded pairlist updated every 25 fs were used for the MD simulations. The temperature was mantained at 300 K using the Berendsen algorithm[51] with a 0.2 ps coupling constant. Four snapshots, extracted every 25 ps from the last 100 ps of MD simulation, were very similar to one another in terms of root-mean-square deviation. An average structure was calculated from the last 100 ps trajectory and energy-minimized using the steepest descent and conjugate gradient methods available within the Sander/Amber to yield the NNBS/(*R*)-**3w** complex shown in Figure 3.

Acknowledgment. The authors thank Italian Ministero della Sanità—Istituto Superiore di Sanità—IX Progetto AIDS 1996 (Grants 40A.0.06 and 9403-59) for financial aid. Acknowledgments are due to Italian MURST (40% funds) and Regione Autonoma Sardegna (Assessorato Sanità) for partial support.

References

(1) De Clercq, E. Targets and Strategies for the Antiviral Chemotherapy of AIDS. *Trends Pharmacol. Sci.* **1990**, *11*, 198−205.
(2) Katz, R. A.; Skalka, A. M. The Retroviral Enzymes. *Annu. Rev. Biochem.* **1994**, *63*, 133−173.
(3) Turner, B. G.; Summers, M. F. Structural Biology of HIV. *J. Mol. Biol.* **1999**, *285*, 1−32.
(4) Mitsuya, H.; Weinhold, K. J.; Furman, P. A.; St. Clair, M. H.; Nusinoff-Lehrman, S.; Gallo, R. C.; Bolognesi, D.; Barry, D. W.; Broder, S. 3′-Azido-3′-deoxythymidine (BW A509U): An Antiviral Agent That Inhibits the Infectivity and Cytopathic Effect of Human T-Lymphotropic Virus Type III/Lymphadenopathy-Associated Virus in Vitro. *Proc. Natl. Acad. Sci. U.S.A.* **1985**, *82*, 7096−7100.

(5) St. Clair, M. H.; Richards, C. A.; Spector, T.; Weinhold, K. J.; Miller, W. H.; Langlois, A. J.; Furman, P. A. 3′-Azido-3′-deoxythymidinetriphosphate as an Inhibitor and Substrate of Purified Human Immunodeficiency Virus Reverse Transcriptase. *Antimicrob. Agents Chemother.* **1987**, *31*, 1972−1977.
(6) Richman, D. D.; Fischi, M. A.; Grieco, M. H.; Gottleib, M. S.; Volberding, P. A.; Laskin, O. L.; Leedom, J. M.; Groopman, J. E.; Mildvan, D.; Hirsch, M. S.; Jackson, G. G.; Durak, D. T.; Nusinoff-Lehrman, S. The Toxicity of Azidothymidine (AZT) in Treatment of Patients with AIDS and AIDS-Related Complex. *N. Engl. J. Med.* **1987**, *317*, 192−197.
(7) Richman, D. D. Resistance of Clinical Isolates of Human Immunodeficiency Virus to Antiretroviral Agents. *Antimicrob. Agents Chemother.* **1993**, *37*, 1207−1221.
(8) Terasaki, T.; Pardridge, W. M. Restricted Transport of 3′-Azido-3′-deoxythymidine and Dideoxynucleosides Through the Blood−Brain Barrier. *J. Infect. Dis.* **1988**, *158*, 630−632.
(9) Merluzzi, V. J.; Hargrave, K. D.; Labadia, M.; Grozinger, K.; Skoog, M.; Wu, J. C.; Shih, C.-K.; Eckner, K.; Hattox, S.; Adams, J.; Rosenthal, A. S.; Faanes, R.; Eckner, R. J.; Koup, R. A.; Sullivan, J. L. Inhibition of HIV-1 Replication by a Nonnucleoside Reverse Transcriptase Inhibitor. *Science* **1990**, *250*, 1411−1413.
(10) Pauwels, R.; Andries, K.; Desmyter, J.; Schols, D.; Kukla, M. J.; Breslin, H. J.; Rayemaeckers, A.; Gelder, J. V.; Woestenborghs, R.; Heykants, J.; Schellekens, K.; Janssen, M. A. C.; De Clercq, E.; Janssen, P. A. J. Potent and Selective Inhibition of HIV-1 Replication in Vitro by a Novel Series of TIBO Derivatives. *Nature* **1990**, *343*, 470−474.
(11) Romero, D. L.; Busso, M.; Tan, C.-K.; Reusser, F.; Palmer, J. R.; Poppe, S. M.; Aristoff, P. A.; Downey, K. M.; So, A. G.; Rasnick, L.; Tarpley, W. G. Nonnucleoside Reverse Transcriptase Inhibitors That Potently and Specifically Block Human Immunodeficiency Virus Type 1 Replication. *Proc. Natl. Acad. Sci. U.S.A.* **1991**, *88*, 8806−8810.
(12) Pauwels, R.; Andries, K.; Debyser, Z.; Van Daele, P.; Schols, D.; Stoffels, P.; De Vreese, K.; Woestenborghs, R.; Vandamme, A.-M.; Janssen, C. G. M.; Anne, J.; Cauwenbergh, G.; Desmyter, J.; Heykants, J.; Janssen, M. A. C.; De Clercq, E.; Janssen, P. A. J. Potent and High Selective HIV-1 Inhibition by a New Series of α-Anilinophenylacetamide α-APA Derivatives Targeted at HIV-1 Reverse Transcriptase. *Proc. Natl. Acad. Sci. U.S.A.* **1993**, *90*, 1711−1715.
(13) Cantrell, A. S.; Engelhardt, P.; Hogberg, M.; Jaskunas, S. R.; Johansson, N. G.; Jordan, C. L.; Kangasmetsa, J.; Kinnick, M. D.; Lind, P.; Morin, J. M., Jr.; Muesing, M. A.; Noreen, R.; Oberg, B.; Prane, P.; Sahlberg, C.; Ternasky, R. J.; Vasileff, R. T.; Vrang, L.; West, S. J.; Zhang, H. Phenethylthiazolylthiourea (PETT) Compounds as a New Class of HIV-1 Reverse Transcriptase Inhibitors. 2. Synthesis and Further Structure−Activity Relationship Studies of PETT Analogues. *J. Med. Chem.* **1996**, *39*, 4261−4274.
(14) Baba, M.; Tanaka, H.; De Clercq, E.; Pauwels, R.; Balzarini, J.; Schols, D.; Nakashima, H.; Perno, C.-F.; Walker, R. T.; Miyasaka, T. Highly Specific Inhibition of Human Immunodeficiency Virus Type-1 by a Novel 6-Substituted Acyclouridine Derivative. *Biochem. Biophys. Res. Commun.* **1989**, *165*, 1375−1381.
(15) Hopkins, A. L.; Ren, J.; Esnouf, R. M.; Willcox, B. E.; Jones, E. Y.; Ross, C.; Miyasaka, T.; Walker, R. T.; Tanaka, H.; Stammers, D. K.; Stuart, D. I. Complexes of HIV-1 Reverse Transcriptase with Inhibitors of the HEPT Series Reveal Conformational Changes Relevant to the Design of Potent Non-Nucleoside Inhibitors. *J. Med. Chem.* **1996**, *39*, 1589−1600.
(16) Ren, J.; Esnouf, R.; Garman, E.; Somers, D.; Ross, C.; Kirby, I.; Keeling, J.; Darby, G.; Jones, Y.; Stuart, D.; Stammers, D. High Resolution Structures of HIV-1 RT from Four RT-Inhibitor Complexes. *Nat. Struct. Biol.* **1995**, *2*, 293−302.
(17) Smerdon, S. J.; Jager, J.; Wang, J.; Kohlstaedt, L. A.; Chirino, A. J.; Friedman, J. M.; Rice, P. A.; Stetz, T. A. Structure of the Binding Site for Nonnucleoside Inhibitors of the Reverse Transcriptase of Human Immunodeficiency Virus Type 1. *Proc. Natl. Acad. Sci. U.S.A.* **1994**, *91*, 3911, 3915.
(18) Ding, J. Das, K.; Tantillo, C.; Zhang, W.; Clark, A. D., Jr.; Jessen, S.; Lu, X.; Hsiou, Y.; Jacobo-Molina, A.; Andries, K.; Pauwels, R.; Moereels, H.; Koymans, L.; Janssen, P. A. J.; Smith, R. H., Jr.; Kroeger Koepke, M.; Michejda, C. J.; Hughes, S. H.; Arnold, E. Structure of HIV-1 Reverse Transcriptase in a Complex with the Non-Nucleoside Inhibitor α-APA R 95845 at 2.8 Å Resolution. *Structure* **1995**, *3*, 365−379.
(19) Ren, J.; Esnouf, R.; Hopkins, A.; Ross, C.; Jones, Y.; Stammers, D.; Stuart, D. The Structure of HIV-1 Reverse Transcriptase Complexed with 9-Chloro-TIBO: Lessons for Inhibitor Design. *Structure* **1995**, *3*, 915−926.
(20) Das, K.; Ding, J. P.; Hsiou, Y.; Clark, A. D.; Moereels, H.; Koymans, L.; Andries, K.; Pauwels, R.; Janssen, P. A. J.; Boyer, P. L.; Clark, P.; Smith, R. H.; Smith, M. B. K.; Michejda, C. J.; Hughes, S. H.; Arnold, E. Crystal Structures of 8-Cl and 9-Cl TIBO Complexed with Wild-Type HIV-1 RT and 8-Cl TIBO Complexed with the Tyr181Cys HIV-1 RT Drug-Resistant Mutant. *J. Mol. Biol.* **1996**, *264*, 1085−1100.
(21) Esnouf, R. M.; Ren, J. S.; Hopkins, A. L.; Ross, C. K.; Jones, E. Y.; Stammers, D. K.; Stuart, D. I. Unique Features of the Complex between HIV-1 Reverse Transcriptase and the Bis-(heteroaryl)piperazine (BHAP) U-90152 Explain Resistance Mutations for this Nonnucleoside Inhibitor. *Proc. Natl. Acad. Sci. U.S.A.* **1997**, *94*, 3984−3989.
(22) Ren, J.; Esnouf, R. M.; Hopkins, A. L.; Warren, J.; Balzarini, J.; Stuart, D. I.; Stammers, D. K. Crystal Strucutures of HIV-1 Reverse Transcriptase in Complex with Carboxanilide Derivatives. *Biochemistry* **1998**, *37*, 14394−14403.
(23) Högberg, M.; Sahlberg, C.; Engelhardt, P.; Noréen, R.; Kangasmetsä, J.; Johnsson, N. G.; Öberg, B.; Vrang, L.; Zhang, H.; Sahlberg, B.-L.; Unge, T.; Lövgren, S.; Fridborg, K.; Bäckbro, K. Urea−PETT Compounds as a New Class of HIV-1 Reverse Transcriptase Inhibitors. 3. Synthesis and Further Structure−Activity Relationship Studies of PETT Analogues. *J. Med. Chem.* **1999**, *42*, 4150−4160.
(24) De Clercq, E. Toward Improved Anti-HIV Chemotherapy: Therapeutic Strategies for Intervention with HIV Infections. *J. Med. Chem.* **1995**, *38*, 2491−2517.
(25) De Clercq, E. Antiviral Therapy for Human Immunodeficiency Virus Infections. *Clin. Microbiol. Rev.* **1995**, *8*, 200−239.
(26) De Clercq, E. The Role of Non-Nucleoside Reverse Transcriptase Inhibitors (NNRTIs) in the Therapy of HIV-1 Infection. *Antivir. Res.* **1998**, *38*, 153−179.
(27) Artico, M.; Massa, S.; Mai, A.; Marongiu, M. E.; Piras, G.; Tramontano, E.; La Colla, P. 3,4-Dihydro-2-alkoxy-6-benzyl-4-oxopyrimidines (DABOs): A New Class of Specific Inhibitors of Human Immunodeficiency Virus Type 1. *Antiviral Chem. Chemother.* **1993**, *4*, 361−368.
(28) Tramontano, E.; Marongiu, M. E.; De Montis, A.; Loi, A. G.; Artico, M.; Massa, S.; Mai, A.; La Colla, P. Characterization of the Anti-HIV-1 Activity of 3,4-Dihydro-2-alkoxy-6-benzyl-5-oxopyrimidines (DABOs), New Non-Nucleoside Reverse Transcriptase Inhibitors. *Microbiologica* **1994**, *17*, 269−279.
(29) Massa, S.; Mai, A.; Artico, M.; Sbardella, G.; Tramontano, E.; Loi, A. G.; Scano, P.; La Colla, P. Synthesis and Antiviral Activity of New 3,4-Dihydro-2-alkoxy-6-benzyl-4-oxopyrimidines (DABOs), Specific Inhibitors of Human Immunodeficiency Virus Type-1. *Antiviral Chem. Chemother.* **1995**, *6*, 1−8.
(30) Mai, A.; Artico, M.; Sbardella, G.; Massa, S.; Loi, A. G.; Tramontano, E.; Scano, P.; La Colla, P. Synthesis and Anti-HIV-1 Activity of Thio Analogues of Dihydroalkoxybenzyloxopyrimidines. *J. Med. Chem.* **1995**, *38*, 3258−3263.
(31) Mai, A.; Artico, M.; Sbardella, G.; Quartarone, S.; Massa, S.; Loi, A. G.; De Montis, A.; Scintu, F.; Putzolu, M.; La Colla, P. Dihydro(alkylthio)naphthyl methyl)oxopyrimidines: Novel Non-Nucleoside Reverse Transcriptase Inhibitors of the *S*-DABO Series. *J. Med. Chem.* **1997**, *40*, 1447−1454.
(32) Mai, A.; Artico, M.; Sbardella, G.; Massa, S.; Novellino, E.; Greco, G.; Loi, A. G.; Tramontano, E.; Marongiu, M. E.; La Colla, P. 5-Alkyl-2-(alkylthio)-6-(2,6-dihalophenylmethyl)-3,4-dihydropyrimidin-4(3*H*)-ones: Novel Potent and Selective Dihydroalkoxybenzyloxopyrimidine Derivatives. *J. Med. Chem.* **1999**, *42*, 619−627.
(33) Unpublished results of docking studies on the *S*-DABO derivative **2f** (Table 3) performed following the computational procedure described in the present paper.
(34) The short 2-methylthio side chain was selected to keep at minimum the number of conformational variables. In each structure, the methyl of the 2-methylthio side chain and the pyrimidine N1 were oriented in a syn disposition.
(35) Pearlman, D. A.; Case, D. A.; Caldwell, J. W.; Ross, W. S.; Cheatham, T. E., III; Debolt, S.; Ferguson, D. M.; Seibel, G. L.; Kollman, P. A. AMBER, a Package of Computer Programs for Applying Molecular Mechanics, Normal-Mode Analysis, Molecular Dynamics and Free Energy Calculations to Simulate the Structural and Energetic Properties of Molecules. *Comput. Phys. Commun.* **1995**, *91*, 1−41.
(36) Pearlman, D. A.; Case, D. A.; Caldwell, J. W.; Ross, W. S.; Cheatham, T. E., III.; Ferguson, D. M.; Seibel, G.; Singh, U. C.; Weiner, P. K.; Kollman, P. A. *AMBER*, version 4.1; Department of Pharmaceutical Chemistry, University of California: San Francisco, CA, 1995.
(37) Quaglia, M. G.; Mai, A.; Sbardella, G.; Artico, M.; Ragno, R.; Massa, S.; Del Piano, D.; Setzu, G.; Doratiotto, S.; Cotechini, V. Chiral Resolution and Molecular Modeling Investigation of *rac*-2-Cyclopentylthio-6-[1-(2,6-difluorophenyl)ethyl]-3,4-dihydro-5-methylpyrimidin-4(3*H*)-one (MC-1047), a Potent Anti-HIV-1 Reverse Transcriptase Agent of the DABO Class. *Chirality* **2001**, *13*, 75−80.
(38) Young, S. D.; Britcher, S. F.; Tran, L. O.; Payne, L. S.; Lumma, W. C.; Lyle, T. A.; Huff, J. R.; Anderson, P. S.; Olsen, D. B.; Carroll, S. S.; Pettibone, D. J.; O'Brien, J. A.; Ball, R. G.; Balani,

S. K.; Lin, J. H.; Chen, I.-W.; Schleif, W. A.; Sardana, V. V.; Long, W. J.; Byrnes, V. W.; Emini, E. A. L-743,726 (DMP-266): A Novel, Highly Potent Nonnucleoside Inhibitor of the Human Immunodeficiency Virus Type 1 Reverse Transcriptase. *Antimicrob. Agents Chemother.* **1995**, *39*, 2602−2605.

(39) Pauwels, R.; Balzarini, J.; Baba, M.; Snoeck, R.; Schols, D.; Herdewijn, P.; Desmyster, J.; De Clercq, E. Rapid and Automated Tetrazolium-Based Assay for the Detection of anti-HIV Compounds. *J. Virol. Methods* **1988**, *20*, 309−321.

(40) *Sybyl Molecular Modelling System*, version 6.2; Tripos, Inc., St. Louis, MO.

(41) Clark, M.; Cramer, R. D., III; Van Opdenbosch, N. Validation of the General Purpose Tripos 5.2 Force Field. *J. Comput. Chem.* **1989**, *10*, 982−1012.

(42) Head, J.; Zerner, M. C. A Broyden−Fletcher−Goldfarb−Shanno Optimization Procedure for Molecular Geometries. *Chem. Phys. Lett.* **1985**, *122*, 264−274.

(43) Bernstein, F. C.; Koetzle, T. F.; Williams, G. J. B.; Meyer, E. F., Jr.; Brice, M. D.; Rodgers, J. R.; Kennard, O.; Shimanouchi, T.; Tasumi, T. The Protein Data Bank: A Computer Based Archival File for Macromolecular Structures. *J. Mol. Biol.* **1977**, *112*, 535−542.

(44) In a previous article (ref 32) we described the docking of **2f** (listed in Table 3 as the α-desmethyl counterpart of **3w**) into the NNBS extracted from the RT/HEPT complex.[16] In the referenced paper **2f** is denoted as **5r′**.

(45) Cornell, W. D.; Cieplak, P.; Bayly, C. I.; Gould, I. R.; Merz, K. M.; Ferguson, D. M.; Spellmeyer, D. C.; Fox, T.; Caldwell, J. W.; Kollman, P. A. A Second Generation Force Field for the Simulation of Proteins, Nucleic Acids, and Organic Molecules. *J. Am. Chem. Soc.* **1995**, *117*, 5179−5197.

(46) Allinger, N. L. Conformational Analysis. 131. MM2. A Hydrocarbon Force Field Utilizing V_1 and V_2 Torsional Terms. *J. Am. Chem. Soc.* **1977**, *99*, 8127−8134 (subsequent versions, e.g., MM2-87, MM2-89, MM2-91).

(47) Jones-Hertzog, K. D.; Jorgensen, W. L. Binding Affinities for Sulfonamide Inhibitors with Human Thrombin Using Monte Carlo Simulations with a Linear Response Method. *J. Med. Chem.* **1997**, *40*, 1539−1549.

(48) Singh, S. B.; Malamas, M. S.; Hohman, T. C.; Nilakantan, R.; Carper, D. A.; Kitchen, D. Molecular Modeling of the Aldose Reductase−Inhibitor Complex Based on the X-ray Crystal Structure and Studies with Single-Site-Directed Mutants. *J. Med. Chem.* **2000**, *43*, 1062−1070.

(49) Dewar, M. J. S.; Zoebisch, E. G.; Healy, E. F.; Stewart, J. J. P. AM1: A New General Purpose Mechanical Molecular Model. *J. Am. Chem. Soc.* **1985**, *107*, 3902−3909.

(50) MOPAC (version 6.0) is available from Quantum Chemistry Program Exchange, No. 455.

(51) Berendsen, H. J. C.; Postma, J. P. M.; van Gunsteren, W. F.; DiNola, A.; Haak, J. R. Molecular Dynamics with Coupling to an External Bath. *J. Chem. Phys.* **1984**, *81*, 3684−3690.

JM010853H